Open Access Full Text Article

ORIGINAL RESEARCH

Enhanced Antitumor Efficacy of Macrophage-Mediated Egg Yolk Lipid-Derived Delivery System Against Breast Cancer

Yanguan Lv[1,*]
Yali Jun[2,*]
Zhuang Tang[2,3,*]
Xiang Li[2]
Mingyue Tao[2,4]
Zhengwei Zhang[5]
Lu Liu[5]
Su'An Sun[5]
Qilong Wang[2]
Chao Luo [iD][2]
Li Zhang[2]

[1]Department of Clinical Medical Laboratory, Huai'an Maternity and Child Healthcare Hospital Affiliated to Yangzhou University Medical Academy, Huai'an 223002, People's Republic of China; [2]Department of Central Laboratory, The Affiliated Huaian No.1 People's Hospital of Nanjing Medical University, Huai'an 223300, People's Republic of China; [3]School of Pharmacy and State Key Laboratory of Quality Research in Chinese Medicines, Macau University of Science and Technology, Macau, 999078, People's Republic of China; [4]Department of Clinical Oncology, The Affiliated Huaian No.1 People's Hospital of Nanjing Medical University, Huai'an 223300, People's Republic of China; [5]Department of Pathology, The Affiliated Huaian No.1 People's Hospital of Nanjing Medical University, Huai'an 223300, People's Republic of China

*These authors contributed equally to this work

Correspondence: Li Zhang; Chao Luo
Department of Central Laboratory, The Affiliated Huaian No.1 People's Hospital of Nanjing Medical University, Huai'an 223300, People's Republic of China
Tel +8615861710452
Email zhangl@njmu.edu.cn;
hayylch@njmu.edu.cn

Background: Chemotherapy is the primary treatment for most cancers apart from surgery. However, the use of chemotherapeutic drugs is limited by side effects and restricted accumulation in tumors because of unique tumor microenvironments. Macrophages have excellent drug delivery potential owing to their chemotaxis and can home in on tumors.

Materials and Methods: We developed an effective drug-delivery system for doxorubicin using macrophages. Doxorubicin-loaded egg yolk lipid-derived nanovectors (EYLNs-Dox) were prepared, EYLNs-Dox-loaded macrophages (Mac/EYLNs-Dox) were developed and their tumor penetration and anti-cancer activity against 4T1 cells were analyzed. The biodistribution and anti-4T1 breast cancer activities were determined using 4T1 subcutaneous and lung metastasis models.

Results: EYLNs-Dox was successfully internalized into macrophages without affecting their viability and was less toxic than Dox. Mac/EYLNs-Dox penetrated the 4T1 tumor spheroids more efficiently and was more effective in inhibiting tumors in vitro. Macrophages significantly enhanced the distribution of EYLNs vectors in both inflammatory and tumor sites, playing a more effective role in the inhibition of tumors.

Conclusion: EYLNs-Dox can be effectively delivered using macrophages and Mac/EYLNs-Dox might be a promising targeted delivery system for breast cancer.

Keywords: macrophage, drug delivery, target therapy, egg yolk lipid-derived nanovector, breast cancer

Introduction

Breast cancer is the most common cancer among women globally. In 2018, a total of 268,670 new cases of breast cancer were diagnosed and with 41,400 deaths, it ranked second as the leading cause of cancer-related deaths.[1] Chemotherapy remains the most commonly used approach for the treatment of breast cancer. Unfortunately, this therapeutic approach is associated with a large number of side effects, such as cardiotoxicity and neurotoxicity.[2,3] A reduction in the off-target side effects of chemotherapeutic drugs would greatly improve the quality of life of breast cancer patients. Various multifunctional drug delivery systems have been exploited to enhance the anti-tumor efficacy of drugs while decreasing their undesirable side effects.

With the development of nanotechnology, several nanomaterials have been considered as candidate drug carriers.[4,5] Such nanovectors change the pharmacokinetic and pharmacodynamic properties of chemotherapeutic drugs and, in particular,

lead to the preferential accumulation of drugs within solid tumors because of the enhanced permeability and retention (EPR) effect.[6,7] However, despite these advantages for nanoparticle-based delivery of medicines, it must overcome numerous obstacles associated with artificially synthesized nanomaterials, including toxicity and immunogenicity. In recent years, endogenous cell-mediated delivery of therapeutic agents to tumor sites has attracted much attention,[8–10] and macrophages have been reported as one of the most promising tumor-targeted biocarriers owing to their strong phagocytic capacity, chemotaxis, and tolerance to chemotherapeutic drugs.[11–13]

In this study, a model anti-cancer chemotherapeutic drug (doxorubicin)-loaded, natural purified egg yolk lipid-derived nanovector (EYLNs-Dox) was developed, EYLNs nanovector has been demonstrated a promising drug carrier due to the low toxicity and strong EPR effect.[14] EYLNs-Dox was internalized in macrophages to prepare a macrophage-based biomimetic drug delivery system (Mac/EYLNs-Dox). The tumor penetration and inhibitory effects of Mac/EYLNs-Dox were evaluated in vitro and the tumor targeting ability and anti-tumor efficacy of Mac/EYLNs-Dox were evaluated using a 4T1 mouse breast cancer model.

Materials and Methods
Materials

Polar/neutral lipid separation kit was obtained from Cell Biolabs Inc. Doxorubicin hydrochloride (Dox) was purchased from Sigma–Aldrich. The DiR dye was obtained from Life Technologies while 4,6-Diamidino-2-phenylindole dihydrochloride (DAPI) was purchased from Southern Biotech. FITC-CD11b and PE-F4/80 antimouse antibodies were purchased from BioLegend. A terminal deoxynucleotidyl transferase dUTP nick-end labeling (TUNEL) staining kit was purchased from Keygen Biotech and the Cell Counting kit-8 (CCK-8) was obtained from KeyGEN BioTECH.

Cell Culture

The luciferase-expressing mouse breast cancer cells (4T1-luciferase) were provided by Prof. Song Chen from the Institute of Medicinal Biotechnology, Jiangsu College of Nursing, China and the use of cell line was approved by the ethics committee of The Affiliated Huaian No.1 People's Hospital of Nanjing Medical University (DW-P-2018-004-01). The cells were maintained in RPMI 1640 medium supplemented with heat-inactivated FBS (10%), penicillin (50 IU/mL), and streptomycin (50 ng/mL), and were cultured in a humidified CO_2 incubator at 37°C.

Mice

Balb/c mice (6–8-week-old) were obtained from the Institute of Comparative Medicine of Yangzhou University. All animal procedures were approved by the Animal Care and Use Committee of The Affiliated Huaian No. 1 People's Hospital of Nanjing Medical University, China. The guidelines GB/T 35,892–2018 was followed for the welfare of the laboratory animals.

Separation and Analysis of Lipids

Lipids were isolated from egg yolks using a polar/neutral lipid separation kit (Cat. #MET-5009-C; Cell Biolabs). The lipid composition was determined on an ACQUITY UPLC CSH C18 column (2.1 mm × 100 mm, 1.7 μm) at 55°C. The mobile phase A was acetonitrile/water (60:40) with 10 mM ammonium formate and 0.1% formic acid, and the mobile phase B was isopropanol/acetonitrile (90:10) with 10 mM ammonium formate and 0.1% formic acid; the flow rate was 400 μL/min. The solvent gradient was as follows: 0–2 min, 40–43% solvent B; 2–2.1 min, 43–50% solvent B; 2.1–12 min, 50–54% solvent B; 12–12.1 min, 54–70% solvent B; 12.1–18 min, 70–99% solvent B; 18–18.1 min, 99–40% solvent B; 18.1–20.0 min, 40% solvent B.

EYLNs and EYLNs-Dox Preparation and Characterization

EYLNs and EYLNs-Dox were prepared according to the protocol described in our previous publication.[14] In brief, dried lipids[phosphatidylcholine (PC, 75.5%), sphingomyelin (SM, 12.7%), lysophosphatidylcholine (LPC, 6.55%), phosphatidylethanolamine (PE, 4.37%), phosphatidylinositol (PI, 0.54%), and phosphatidylglycerol (PG, 0.34%)] were suspended in distilled water (200–400 μL) and Dox solution (1 mg/mL), respectively, and the suspension was sonicated for 15–20 min using an FS60 bath sonicator (Fisher Scientific). The non-loaded Dox was removed by centrifugation at 100,000 × g for 30 min. Thereafter, the morphology, size and surface zeta potential of EYLNs and EYLNs-Dox were characterized by transmission electron microscope (TEM, FEI Tecnai G2 Spirit BioTwin) and dynamic light scattering (PSS Z3000).

To prepare DiR dye labeled EYLNs, EYLNs vectors were incubated with DiR dye (5 mmol/L) at 37°C for 30 min; then, the free DiR dye was removed by centrifugation at 100,000 × g for 30 min.

Isolation and Identification of Mouse Peritoneal Macrophages

For acquisition of inflammatory macrophages, 1 mL of 6% Brewer thioglycolate medium was injected into the enterocoelia of mice, 4 days prior to the cell harvest. The mice were then euthanized and intraperitoneally injected with 5 mL of harvest medium sterilized PBS with 3% fetal bovine serum. After 30 min, peritoneal fluid was collected and centrifuged for 10 min at 400×g and the cells were resuspended in PBS.

The macrophages were identified by CD11b/F4/80 staining. For immunofluorescent staining, cells were cultured on slides and incubated with anti-mouse CD11b and F4/80 antibodies at 4°C for 1 h; after washing with PBS for three times, the cells were stained with fluorescent dye-labeled secondary antibodies at 37°C for 30 min. The expression of CD11b and F4/80 was analyzed by confocal microscope (NIKON A1). For evaluation of purity, cells were stained with FITC-CD11b and PE-F4/80 antibodies and analyzed by flow cytometry (BD, USA).

Preparation of Mac/EYLNs-Dox

Macrophages under regular culture conditions were treated with Dox or EYLNs-Dox (20 μg/mL Dox) for 1, 3, 6, 12, and 24 h. The loaded macrophages were pelleted by centrifugation. The internalization of Dox or EYLNs-Dox was visualized by imaging using a fluorescent microscope (Leica, DM6B) and the internalized amount was quantified by flow cytometry (BD C6 plus).

Viability of Macrophages

As described above, macrophages were treated with Dox or EYLNs-Dox (20 μg/mL Dox) for 1, 3, 6, 12, 24, and 48 h. The viability of macrophages was assayed using the CCK-8 kit, following the instructions provided by the manufacturer.

Transwell Chemotaxis Assay

In the lower chamber of a 24-well Transwell plate 4T1 cells were cultured at a density of $5×10^4$ cells/well. EYLNs-Dox loaded macrophages (Mac/EYLNs-Dox) were then inoculated in the Transwell inserts and co-cultured for 3, 6 and 12 h. The presence of Dox in 4T1 cells was visualized at different time points using a confocal microscope.

The viability of 4T1 cells in the lower chamber was determined by the CCK-8 assay and apoptosis was detected by TUNEL staining.

Soft Agar Assay

Soft agar assay was performed as described previously.[15] In brief, 4T1 cells were suspended in 0.3% agar prepared in DMEM supplemented with 20% FBS and plated on a layer of 0.6% agar prepared in the same medium.

To assess the tumor penetration capability of Mac/EYLNs-Dox, tumor spheroids were, respectively, treated with Dox, EYLNs-Dox, and Mac/EYLNs-Dox for 6 h, and the Dox signal from 4T1 cells was observed using a fluorescent microscope. To evaluate the anti-tumor activity, tumor spheroids were, respectively, treated with PBS, Dox, EYLNs-Dox, and Mac/EYLNs-Dox every 5 days for 5 times. After 21daysof culture, the tumor cell colonies were photographed and counted. The size of 20 randomly chosen colonies per well was measured and calculated using the formula: Size of colony = (length + width)/2.

In vivo Imaging

A 4T1 murine breast cancer model was established to study the targeted delivery of macrophages. DiR dye-labeled EYLNs (DiR-EYLNs), macrophage-carried DiR-EYLNs (DiR-Mac/EYLNs), and DiR-EYLNs-Dox (DiR-Mac/EYLNs-Dox) were intravenously injected into 4T1-bearing mice; the mice were then sacrificed and the DiR signal in each organ was collected using an image station (Ex:720 nm, Em:790 nm, FX Pro; Bruker) and quantified using the software provided by the vendor.

To monitor tumor growth in vivo, luciferase-labeled tumor 4T1-bearing mice were treated with PBS, Dox, EYLNs-Dox, or Mac/EYLNs-Dox. The luciferase signal was monitored every 5 days using the Bruker FX Pro imaging system. Before scanning, mice were intraperitoneally injected with the luciferase substrate D-luciferin (150 mg/kg in 100 μL of PBS) for 5 min.

Dox Distribution Analysis

Free Dox, EYLNs-Dox, or Mac/EYLNs-Dox was intravenously injected into 4T1-bearing mice at a single dose of 5 mg/kg. Mice in each group were sacrificed at 6 h, 12 h, and 24 h post-injection. The tumors and major organs, including the heart, liver, spleen, lung, and kidney were

removed and the level of Dox in each organ was quantified by HPLC.

Tumor Models

The 4T1 subcutaneous and lung metastasis models were used to determine the anti-cancer activity of Mac/EYLNs-Dox. For the in-situ tumor model, murine 4T1 breast cancer cells (2×10^5) were injected in the mammary fat pads of 6-week-old female BALB/c mice. For the lung metastasis model, 6-week-old female BALB/c mice were intravenously injected with 4T1-luciferase cells (1×10^5).

In vivo Anticancer Efficacy Analysis

After the tumors reached a volume of ~100 mm³, 4T1-bearing mice were randomly divided into 4 groups and were treated with PBS, Dox (5 mg/kg), EYLNs-Dox (5 mg/kg Dox), and Mac/EYLNs-Dox (5 mg/kg) every 6 days for a total of five times. Tumor size and mice weight were measured every 3 days. The tumor volume was calculated according to the formula: volume= $(L \times W^2)/2$. The mice were euthanized, and tumors were collected when the average tumor volume in the control group was over 1000 mm³. The heart, liver, spleen, lung, and kidney were excised and embedded in paraffin for hematoxylin and eosin (H&E) staining.

For lung metastasis model, mice were randomly divided into four groups 5 days after injection with 4T1-luciferase cells and were treated with PBS, Dox (5 mg/kg), EYLNs-Dox (5 mg/kg Dox), and Mac/EYLNs-Dox (5 mg/kg) every 5 days for a total of five times. Luciferase signals were detected every 5 days using the Bruker FX Pro imaging system. The mice were euthanized, and lungs were removed, photographed, and embedded in paraffin for H&E staining.

H&E Staining

To evaluate the biosafety and therapeutic effects of Mac/EYLNs-Dox, liver, lung, heart, spleen, and kidney from tumor-bearing mice were fixed overnight in 4% paraformaldehyde and embedded in paraffin; this was followed by staining of 5 μm tissue sections with H&E.

Statistical Analysis

Data are expressed as means ± standard deviation. Statistical analysis was performed using the GraphPad Prism software (version 7.0). An unpaired *t*-test or one-way analysis of variance followed by the Tukey–Kramer test was performed for multiple group comparisons. Differences were considered statistically significant at *$p < 0.05$.

Results

Preparation and Characterization of EYLNs and EYLNs-Dox

Natural lipids, including phosphatidylcholine, sphingomyelin, lysophosphatidylcholine, phosphatidylethanolamine, phosphatidylinositol, and phosphatidylglycerol, were isolated from egg yolk and the lipid composition was determined (Figure 1A). The lipids were then assembled into nanosized vector-EYLNs. The morphology of EYLNs and Dox-loaded EYLNs (EYLNs-Dox) was examined by TEM. As shown in Figure 1B, EYLNs and EYLNs-Dox exhibited uniform sizes of ~50 and ~90 nm. The Dox encapsulation efficiency was about 75% (Figure 1C). The size (Figure 1D) and surface zeta potential (Figure 1E) of EYLNs and EYLNs-Dox were measured by DLS; the average size and average zeta potential of EYLNs were 50 nm and −45 mV and that of EYLNs-Dox were 90 nm and −35 mV, respectively.

Preparation and Characterization of Mac/EYLNs-Dox

The peritoneal macrophages from mice were isolated and identified by CD11b, F4/80 staining (Figure 2A). The purity of the macrophage preparation was quantified to be higher than 90% (Figure 2B). The Mac/EYLNs-Dox was obtained by incubating the purified macrophages with EYLNs-Dox and the delivery system was imaged using a fluorescent microscope (Figure 2C). We further tested the viability of macrophages after they were loaded with EYLNs-Dox. The viability of macrophages was significantly suppressed after incubating for 6 h (Figure 2D) and the toxicity of EYLNs-Dox was lower than Dox (Figure 2E, *$p < 0.05$ and **$p < 0.01$). The uptake of EYLNs-Dox by macrophages was not time dependent (Figure 2F and G). The uptake reached saturation after 6 h of incubation (Figure 2G).

Cytotoxicity of Dox Released from Mac/EYLNs-Dox

The transwell chemotaxis assay performed to test the release of Dox from Mac/EYLNs-Dox showed that the release of Dox was gradually increased in the Transwell inserts and the drug was taken up by the 4T1 cells in the lower chamber (Figure 3A). The viability of 4T1 cells was subsequently determined by the CCK-8 assay and the rate of apoptosis was analyzed by TUNEL staining. The
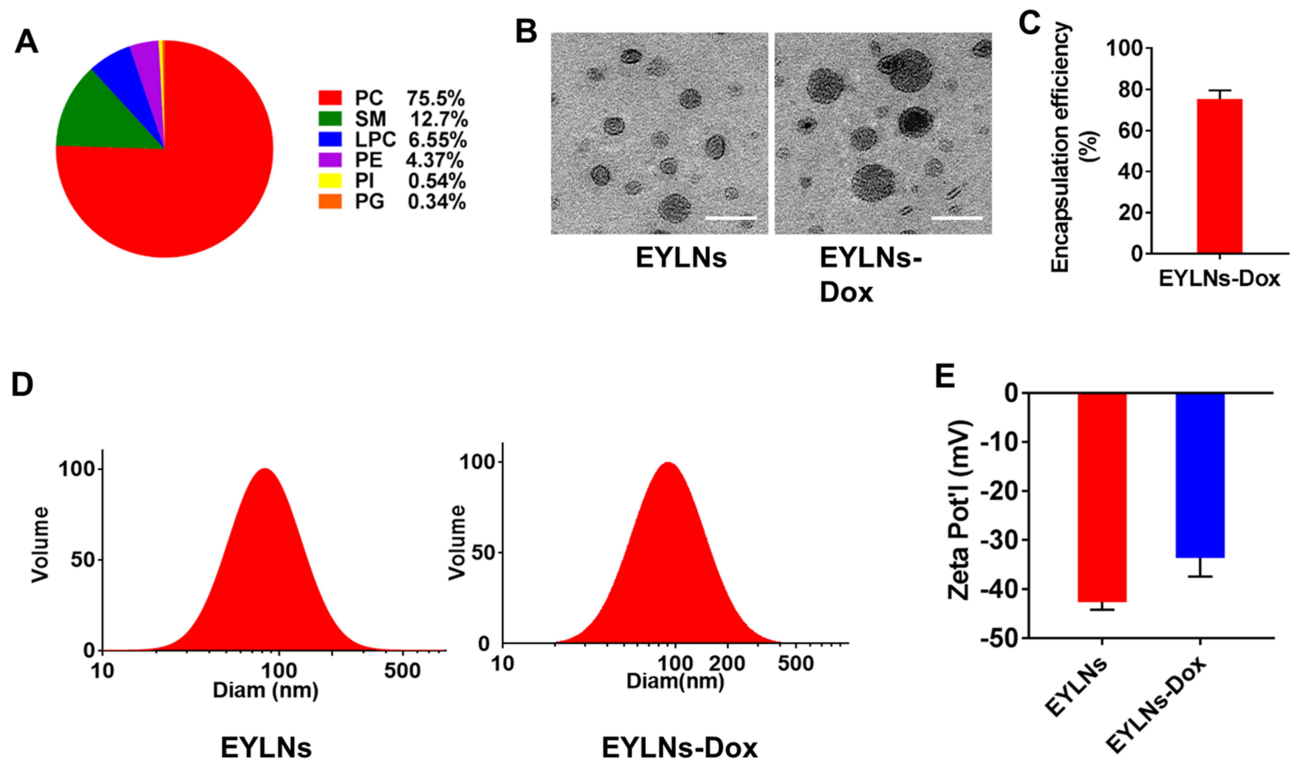
Figure 1 Lipids isolation, lipids derived nanovectors preparation and characterization. (**A**) Composition analysis of isolated lipids from egg yolk. (**B**) TEM imaging of EYLNs and EYLNs-Dox. (**C**) Encapsulation efficiency of Dox by EYLNs. (**D**) Size distribution of EYLNs and EYLNs-Dox. (**E**) Zeta potentials of EYLNs and EYLNs-Dox by dynamic light scattering. Scale bar: 100 nm.
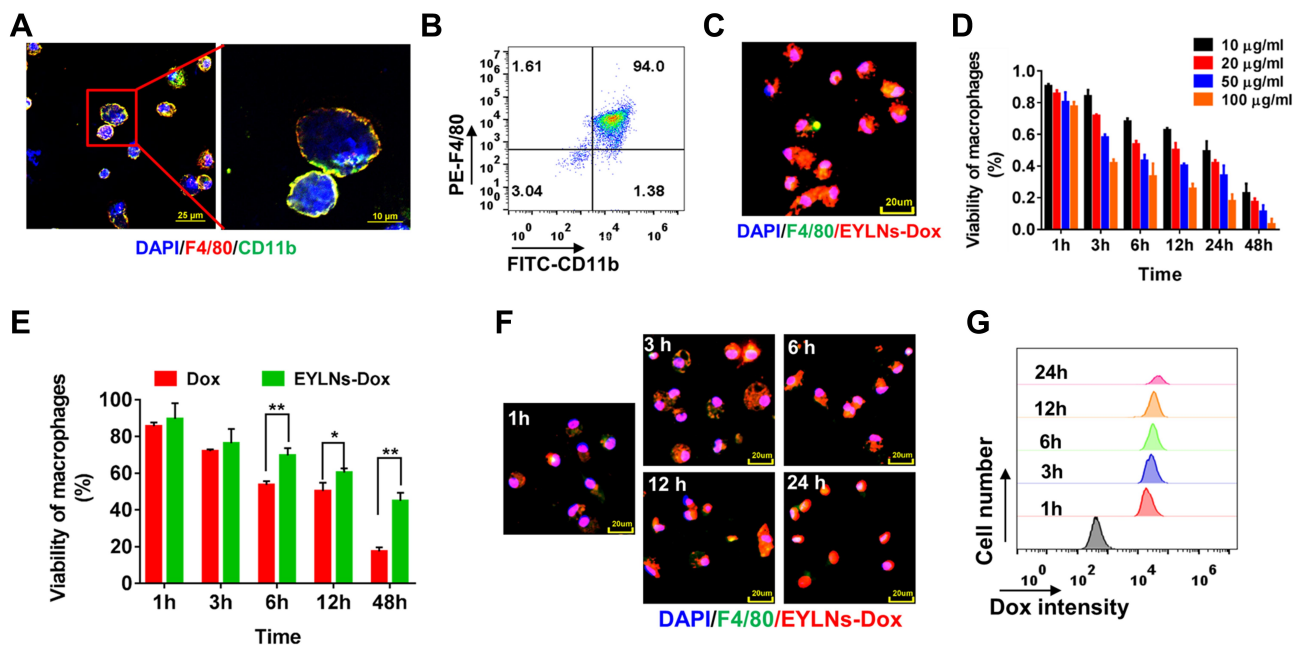

Figure 2 Purification of peritoneal macrophages and preparation of EYLNs-Dox loaded macrophages (Mac/EYLNs-Dox). (**A**) Identification of peritoneal macrophages by staining with F4/80 and CD11b. (**B**) FACS analyzing the purity of peritoneal macrophages by FITC-CD11b and PE-F4/80 staining. (**C**) Observation of Mac/EYLNs-Dox by immunofluorescence staining. (**D**) Viability of macrophages after incubation with EYLNs-Dox (10, 20, 50, 100 mg/mL) for different time (1, 3, 6, 12, 24 and 48 h). (**E**) Viability of macrophages after respectively incubation with Dox and EYLNs-Dox. Uptake efficiency detection of EYLNs-Dox by macrophages via (**F**) immunofluorescence staining and (**G**) flow cytometry. Scale bar: 20 μm and 25 μm. *$p<0.05$ and **$p<0.01$.
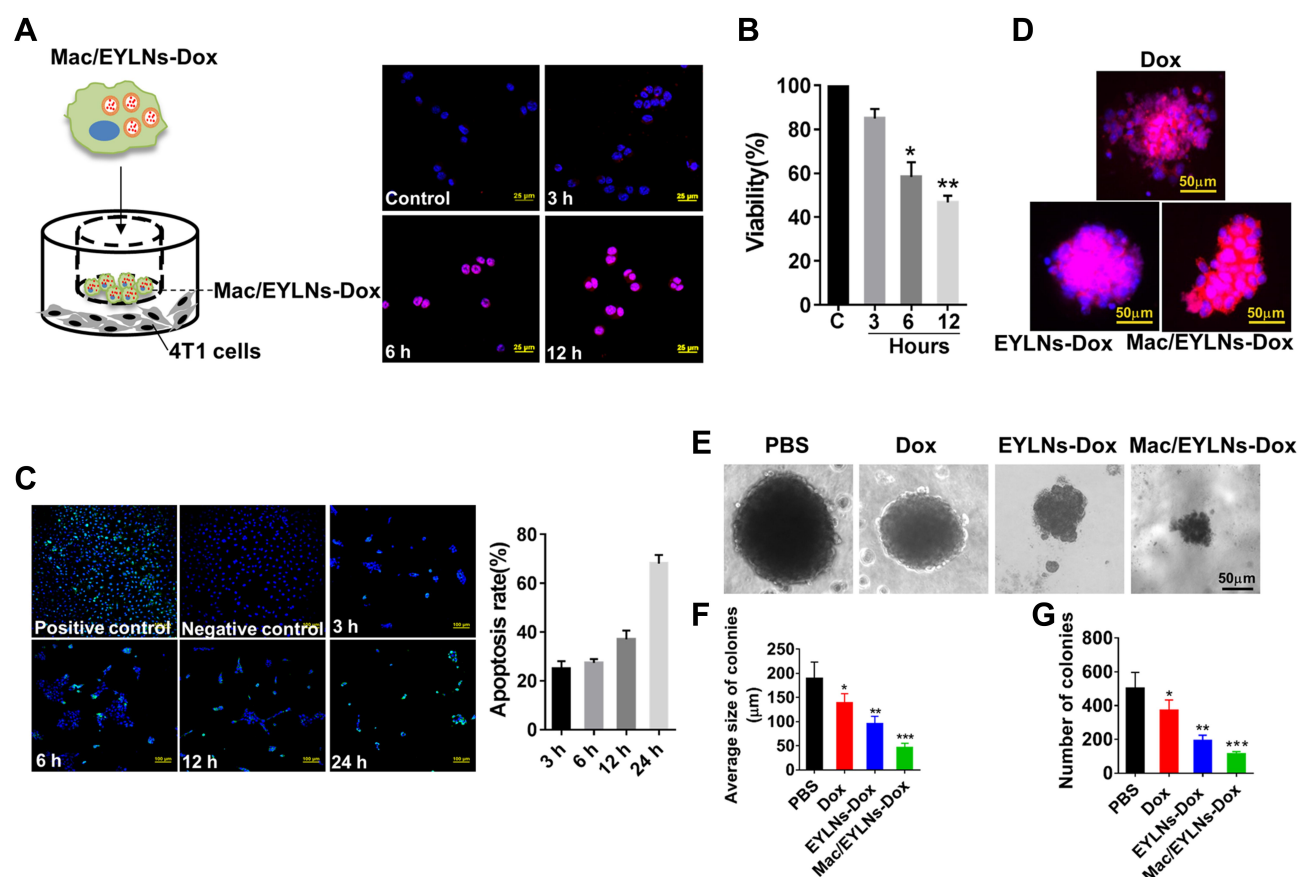
Figure 3 Transmigration capability and in vitro cytotoxicity of Mac/EYLNs-Dox. (**A**) Macrophages were loaded with EYLNs-Dox and cultured for 3, 6, 12 h in the Transwell inserts with 4T1 cells in the lower chambers. Dox signals in 4T1 cells were analyzed by confocal imaging. The viability (**B**) and apoptosis (**C**) of 4T1 cells in the lower chamber after culturing for 3, 6, 12 and 24 h. (**D**) Penetration of Mac/EYLNs-Dox into 3D 4T1 spheroids. (**E**) 4T1 spheroids were treated with PBS, Dox, EYLNs-Dox and Mac/EYLNs-Dox every 5 days for 5 times. After 21-day culturing, the colonies of tumor cells were photographed. The average size (**F**) of chosen colonies was calculated and the numbers (**G**) were counted. *$p < 0.05$, **$p < 0.01$ and ***$p < 0.001$. Scale bar: 25 μm, 50 μm and 100 μm.

viability of 4T1 cells was strikingly inhibited by Dox released from Mac/EYLNs-Dox in a time-dependent manner (*$p < 0.05$, **$p < 0.01$) (Figure 3B). TUNEL data also revealed that the proportion of apoptotic 4T1 cells was increased in a time-dependent manner (Figure 3C).

The tumor-penetration ability of Mac/EYLNs-Dox was evaluated using a multicellular 4T1 tumor spheroid model. After incubation for 6 h, the Dox signal in the spheroids was visualized using a fluorescent microscope. Mac/EYLNs-Dox was more capable of permeating the tumor than was either EYLNs-Dox or Dox (Figure 3D). The growth of tumor spheroids was the most significantly suppressed by Mac/EYLNs-Dox (Figure 3E–G, *$p < 0.05$, **$p < 0.01$ and ***$p < 0.001$).

Biodistribution of Mac/EYLNs-Dox

To investigate the in vivo distribution of Mac/EYLNs-Dox, 4T1 tumor-bearing mice were intravenously injected with DiR-EYLNs-Dox and DiR-Mac/EYLNs-Dox. It was

observed that the distribution of EYLNs-Dox in 4T1 tumors was dramatically enhanced when they were loaded in macrophages (Figure 4A and B *$p < 0.05$) and the accumulation process was time dependent (Figure 4C). The amount of Dox in tumor tissues was quantified and its distribution was found to be consistent with that in the case of Mac/EYLNs-Dox (Figure 4D, *$p < 0.05$, **$p < 0.01$).

Therapeutic Effect of Mac/EYLNs-Dox in vivo

The antitumor efficacy of Mac/EYLNs-Dox was first investigated using the subcutaneous 4T1 murine breast cancer model. The tumor-bearing mice were randomly divided into four groups and treated with PBS, Dox, EYLNs-Dox, or Mac/EYLNs-Dox (at an identical dose of 5 mg/kg Dox in the case of the last three groups), every 6 days for five times. Mac/EYLNs-Dox exerted a more effective antitumor effect when compared with
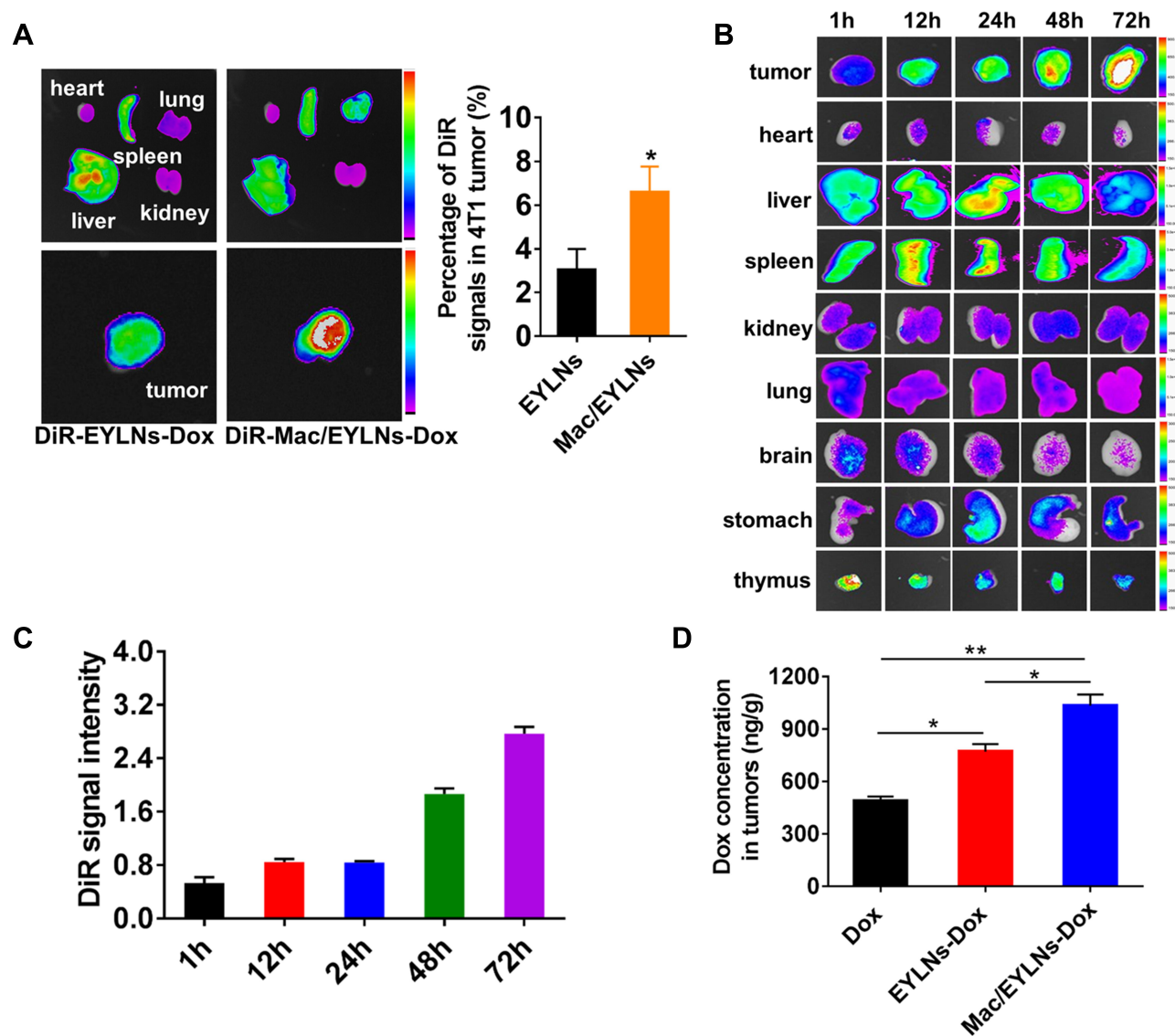
Figure 4 Biodistribution of Mac/EYLNs-Dox and Dox in 4T1-bearing tumor mice. (**A**) DiR dye labeled EYLNs-Dox and Mac/EYLNs-Dox were respectively I.V. injected into 4T1-bearing tumor mice for 24 h, then the DiR dye signals in mice organs and tumors were scanned and analyzed by Bruker FX Pro imaging system and the DiR signals in tumors were quantified. (**B**) DiR-Mac/EYLNs-Dox was I.V. injected into 4T1 tumor mice and the accumulation of Mac/EYLNs-Dox in tumors and other organs was imaged at different time point (1, 12, 24, 48, 72 h) and the DiR signal intensity (**C**) was calculated. (**D**) 4T1 tumor mice were treated with Mac/EYLNs-Dox and the distribution of Dox in tumors was detected by HPLC. *$p<0.05$, **$p<0.01$.

Dox and EYLNs-Dox (Figure 5A and B). We also established the 4T1 lung metastasis model to further test the antitumor efficacy of Mac/EYLNs-Dox. Balb/c mice were intravenously injected with 4T1-luciferase cells, and after 5 days, the mice were treated five times with PBS, Dox, EYLNs-Dox, or Mac/EYLNs-Dox, every 5 days. The luciferase signals were scanned every 5 days. It was observed that the metastasis of 4T1 cells was effectively suppressed by EYLNs-Dox and Mac/EYLNs-Dox, especially by the latter to a greater extent (Figure 5C and D, *$p<0.05$, **$p<0.01$). There were several tumor nodules in the lungs of mice in the PBS group, and the metastatic

nodules were also visible in the lungs of mice treated with Dox and EYLNs-Dox. In the Mac/EYLNs-Dox group, an insignificant number of tumor nodules was observed (Figure 5E). Metastasis was also examined by histopathological examination, wherein Mac/EYLNs-Dox showed the most effective anti-metastatic ability (Figure 5F).

Discussion

Nanomaterial-mediated drug delivery has become one of the most promising strategies for cancer therapy. Different types of nanomaterials, including liposomes,[16] polymers,[17] silica,[18] metals,[19,20] and carbon nanomaterials,[21] have been
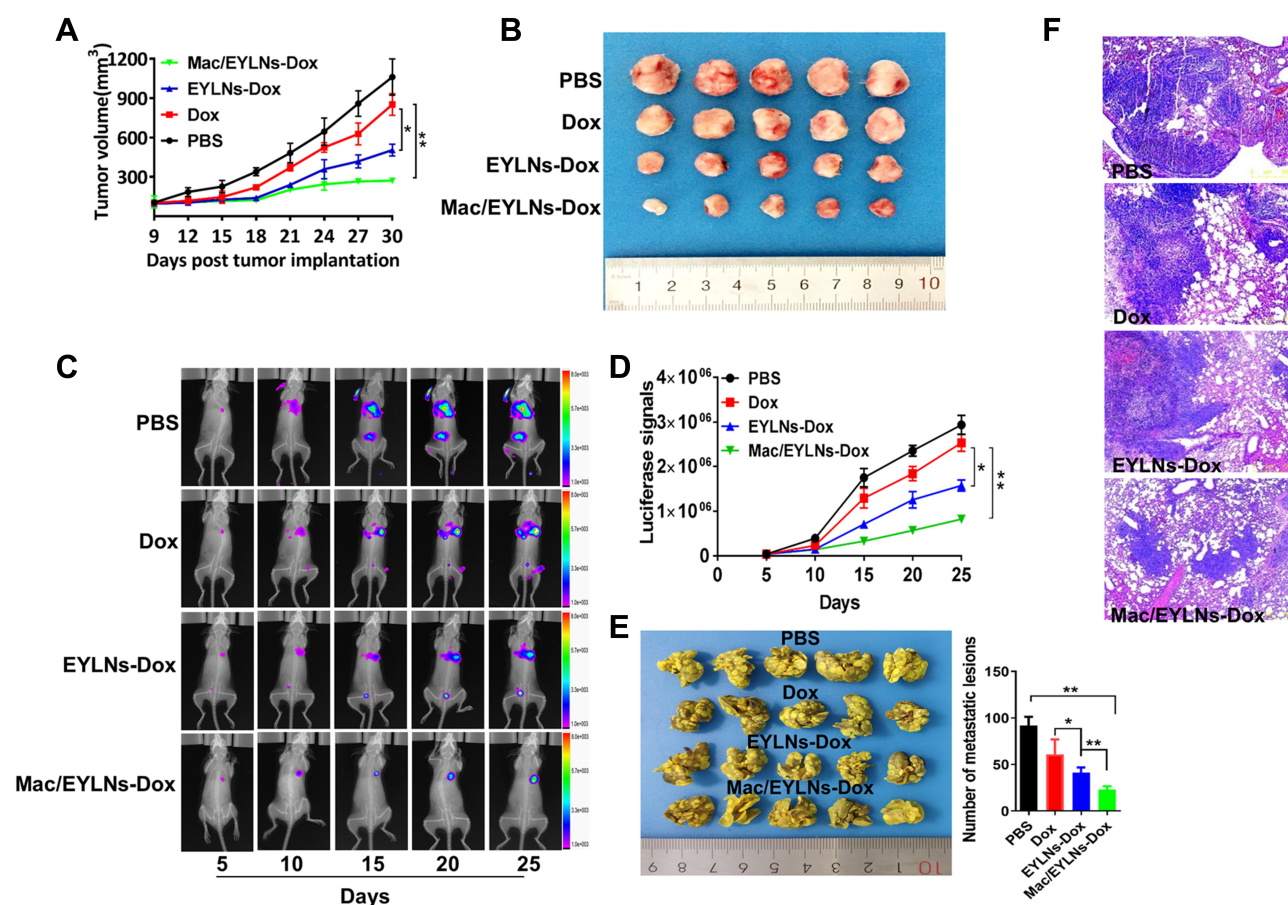
Figure 5 Therapeutic effects of Mac/EYLNs-Dox on 4T1 tumors. Subcutaneous implant 4T1 tumor mice were treated with PBS, Dox, EYLNs-Dox and Mac/EYLNs-Dox, (**A**) tumor growth was recorded every 3 days. (**B**) Mice were sacrificed 30 days after treatment, tumors were removed and photographed. (**C**) 4T1 lung metastasis model was established and treated with PBS, Dox, EYLNs-Dox and Mac/EYLNs-Dox every 5 days for 5 times, the metastatic tumors were detected by in vivo imaging and the tumor signals were quantified (**D**). After 5 times treatment, mice were sacrificed and the lungs were removed, stained with and photographed (**E**), the pathology of lungs was analyzed by HE staining (**F**). $*p<0.05$, $**p<0.01$. Scale bar: 500µm.

extensively explored over the decades for their biomedical applications. However, most of the nanomaterials are still at the research stage and have not been translated from laboratory to the market. Only a few nanomaterials have been clinically approved for medical applications by the US FDA. The major challenges associated with synthetic nanomaterials are biocompatibility and potential toxicity.

To overcome the aforementioned limitations of nanomaterials, increasing number of studies focus on the development of novel nanomaterials with low toxicity, reduced immune rejection, and better biodistribution. Engineering of biomimetic drug delivery system has especially been one of the most researched strategies. Delivery of nanoparticles coated with cell membrane is one of the most important and effective tactics. Various cell membranes, such as those of erythrocytes,[22] platelets,[23] white blood cells,[24] macrophages,[25] and cancer cells,[26] have been employed for coating nanoparticles. Cell membrane

coating affects nanodrugs in many ways; for instance, this can enhance immune evasion, reduce renal clearance after uptake through the reticuloendothelial system, prolong circulation time, and increase the target distribution of nanodrugs.[27] However, the research in this field is still in its preclinical stage and several challenges have to be overcome before clinical translation of this strategy from bench to the bedside. The major challenges are the reproducibility of membrane composition and the stability of membrane coated on the nanomaterials. In the light of above-mentioned vulnerabilities, immune cells have been exploited as new drug delivery vehicles. Immune cells, including mononuclear phagocytes and neutrophils, possess strong mobility and can migrate across impermeable barriers, thus, release drugs in the inflammatory or tumor tissues.[8,28]

Macrophages are specialized cells involved in the detection, phagocytosis, and destruction of harmful organisms.

The extremely strong phagocytic ability and chemotaxis in response to inflammation make macrophages an excellent candidate for drug delivery. Fu constructed a biomimetic delivery system by loading Dox into a mouse macrophage-like cell line, RAW264.7, and demonstrated that the Dox-loaded macrophages showed more promising anti-breast cancer activities than did doxorubicin.[29] More importantly, studies by Qiang indicated that macrophages could be protected from the toxicity of Dox by loading with the nanocarrier. They developed a RAW264.7-mediated delivery system by encapsulating Dox-loaded reduced graphene oxide (MAs-DOX/PEG-BPEI-rGO) and found that compared with free Dox, RAW264.7 cells could absorb more DOX/PEG-BPEI-rGO. Moreover, both in vitro and in vivo tests demonstrated that MAs-DOX/PEG-BPEI-rGO exhibited a significant inhibitory effect on the growth of prostate cancer.[30] In contrast to the above studies, Choi established mouse peritoneal macrophage bearing liposomal Dox (macrophage-LP-Dox), and using the subcutaneous and metastatic xenograft lung cancer models confirmed that the generated nanomaterials inhibited tumor growth more effectively than did Dox and LP-Dox. They also indicated that monocytes and macrophages from cancer patients might be suitable candidates for personalized drug administration.[31]

In the present study, we developed a Dox encapsulated, natural egg yolk lipids derived nanovector (EYLNs-Dox) and constructed a macrophage-mediated biomimetic delivery system (Mac/EYLNs-Dox) by incubating EYLNs-Dox with purified peritoneal macrophages. Consistent with the results of previous studies, our data confirm that EYLNs-Dox can be loaded into peritoneal macrophages with high efficiency, and dramatically enhance in vitro tumor inhibition by improving the penetration of Dox. Furthermore, the distribution of EYLNs-Dox in 4T1 tumors was significantly increased upon loading in macrophages; 4T1 tumor growth and metastasis was most effectively suppressed by Mac/EYLNs-Dox. Besides, nanovector-EYLNs prepared from natural purified egg yolk lipids displays good biocompatibility and low toxicity (data not shown). This is another crucial characteristic of the Mac/EYLNs-Dox delivery system for effective clinical translation and is also the major difference from most of other macrophage-mediated drug delivery systems described earlier.

Conclusion

We report a peritoneal macrophage-mediated biomimetic drug delivery system (Mac/EYLNs-Dox) that utilizes the physiological characteristics of macrophages to transport Dox-loaded natural egg yolk derived nanovector (EYLNs-Dox) to tumor sites. Using several experiments, we validated that the penetration of EYLNs-Dox was obviously enhanced and the distribution of EYLNs-Dox in 4T1 tumors was remarkably increased by loading into the macrophages. Further experiments confirmed that Mac/EYLNs-Dox exert a more potent anticancer effect than does EYLNs-Dox or Dox. This study provides a valuable tool for therapeutic drug delivery.

Acknowledgments

Disclosure

The authors declare no conflicts of interest in this work.

References

1. Siegel RL, Miller KD, Jemal A. Cancer statistics, 2018. *CA Cancer J Clin*. 2018;68(1):7–30. doi:10.3322/caac.21442
2. Qi L, Luo Q, Zhang Y, Jia F, Zhao Y, Wang F. Advances in toxicological research of the anticancer drug cisplatin. *Chem Res Toxicol*. 2019;32(8):1469–1486. doi:10.1021/acs.chemrestox.9b00204
3. Xia P, Liu Y, Chen J, Coates S, Liu DX, Cheng ZK. Inhibition of cyclin-dependent kinase protects against doxorubicin-induced cardiomyocyte apoptosis and cardiomyopathy. *J Biol Chem*. 2018;293 (51):19672–19685. doi:10.1074/jbc.RA118.004673
4. Patra JK, Das G, Fraceto LF, et al. Nano based drug delivery systems: recent developments and future prospects. *J Nanobiotechnol*. 2018;16 (1):71. doi:10.1186/s12951-018-0392-8
5. Ankita D, Ashish B, Raj KN. Nanoparticles as carriers for drug delivery in cancer. *Artif Cells Nanomed Biotechnol*. 2018;46 (sup2):295–305. doi:10.1080/21691401.2018.1457039
6. Kalyane D, Raval N, Maheshwari R, Tambe V, Kalia K, Tekade RK. Employment of enhanced permeability and retention effect (EPR): nanoparticle-based precision tools for targeting of therapeutic and diagnostic agent in cancer. *Mater Sci Eng C Mater Biol Appl*. 2019;98:1252–1276. doi:10.1016/j.msec.2019.01.066
7. Golombek SK, May JN, Theek B, et al. Tumor targeting via EPR: strategies to enhance patient responses. *Adv Drug Deliv Rev*. 2018;130:17–38. doi:10.1016/j.addr.2018.07.007
8. Xue J, Zhao Z, Zhang L, et al. Neutrophil-mediated anticancer drug delivery for suppression of postoperative malignant glioma recurrence. *Nat Nanotechnol*. 2017;12(7):692–700. doi:10.1038/nnano.2017.54
9. Han H, Eyal S, Portnoy E, et al. Monocytes as carriers of magnetic nanoparticles for tracking inflammation in the epileptic rat brain. *Curr Drug Deliv*. 2019;16(7):637–644. doi:10.2174/15672018166661 90619122456

10. Han Y, Zhao R, Neutrophil-Based Delivery XF. Systems for nanotherapeutics. *Small*. 2018;14(42):e1801674. doi:10.1002/smll.201801674

11. Evans MA, Huang P, Iwamoto Y, et al. Macrophage-mediated delivery of light activated nitric oxide prodrugs with spatial, temporal and concentration control. *Chem Sci*. 2018;9(15):3729–3741. doi:10.1039/c8sc00015h

12. Choi MR, Stanton-Maxey KJ, Stanley JK, et al. A cellular trojan horse for delivery of therapeutic nanoparticles into tumors. *Nano Lett*. 2007;7(12):3759–3765. doi:10.1021/nl072209h

13. Liu R, An Y, Jia WF, et al. Macrophage-mimic shape changeable nanomedicine retained in tumor for multimodal therapy of breast cancer. *J Control Release*. 2020;321:589–601. doi:10.1016/j.jconrel.2020.02.043

14. Tang Z, Luo C, Jun YL, et al. Nanovector assembled from natural egg yolk lipids for tumor-targeted delivery of therapeutics. *ACS Appl Mater Interfaces*. 2020;12(7):7984–7994. doi:10.1021/acsami.9b22293

15. Luo C, Shu Y, Luo J, et al. Intracellular IL-37b interacts with Smad3 to suppress multiple signaling pathways and the metastatic phenotype of tumor cells. *Oncogene*. 2017;36(20):2889–2899. doi:10.1038/onc.2016.444

16. Xing H, Hwang KV, Lu Y. Recent developments of liposomes as nanocarriers for theranostic applications. *Theranostics*. 2016;6(9):1336–1352. doi:10.7150/thno.15464

17. Khandare J, Calderón M, Dagia NM, Haag R. Multifunctional dendritic polymers in nanomedicine: opportunities and challenges. *Chem Soc Rev*. 2012;41(7):2824–2848. doi:10.1039/c1cs15242d

18. Zhang Y, Hsu BY, Ren CJ, Li X, Wang J. Silica-based nanocapsules: synthesis, structure control and biomedical applications. *Chem Soc Rev*. 2015;44(1):315–335. doi:10.1039/c4cs00199k

19. Kim B, Han G, Toley BJ, Kim CK, Rotello VM, Forbes NS. Tuning payload delivery in tumour cylindroids using gold nanoparticles. *Nat Nanotechnol*. 2010;5(6):465–472. doi:10.1038/nnano.2010.58

20. Ling D, Lee N, Hyeon T. Chemical synthesis and assembly of uniformly sized iron oxide nanoparticles for medical applications. *Acc Chem Res*. 2015;48(5):1276–1285. doi:10.1021/acs.accounts.5b00038

21. Loh KP, Ho D, Chiu GNC, Leong DT, Pastorin G, Chow EK. Clinical applications of carbon nanomaterials in diagnostics and therapy. *Adv Mater*. 2018;30(47):e1802368. doi:10.1002/adma.201802368

22. Guo YY, Wang D, Song QL, et al. Erythrocyte membrane-enveloped polymeric nanoparticles as nanovaccine for induction of antitumor immunity against melanoma. *ACS Nano*. 2015;9(7):6918–6933. doi:10.1021/acsnano.5b01042

23. Ying M, Zhuang J, Wei XL, et al. Remote-loaded platelet vesicles for disease-targeted delivery of therapeutics. *Adv Funct Mater*. 2018;28(22):1801032. doi:10.1002/adfm.201801032

24. Wang QL, Ren Y, Mu JY, et al. Grapefruit-derived nanovectors use an activated leukocyte trafficking pathway to deliver therapeutic agents to inflammatory tumor sites. *Cancer Res*. 2015;75(12):2520–2529. doi:10.1158/0008-5472.CAN-14-3095

25. Hu C, Lei T, Wang YZ, et al. Phagocyte-membrane-coated and laser-responsive nanoparticles control primary and metastatic cancer by inducing anti-tumor immunity. *Biomaterials*. 2020;255:120159. doi:10.1016/j.biomaterials.2020.120159

26. Sun HP, Su JH, Meng QS, et al. Cancer-cell-biomimetic nanoparticles for targeted therapy of homotypic tumors. *Adv Mater*. 2016;28(43):9581–9588. doi:10.1002/adma.201602173

27. Luk BT, Zhang LF. Cell membrane-camouflaged nanoparticles for drug delivery. *J Control Release*. 2015;220:600–607. doi:10.1016/j.jconrel.2015.07.019

28. Sathyamoorthy N, Dhanaraju MD. Shielding therapeutic drug carriers from the mononuclear phagocyte system: a review. *Crit Rev Ther Drug Carrier Syst*. 2016;33(6):489–567. doi:10.1615/CritRevTherDrugCarrierSyst.2016012303

29. Fu JJ, Wang D, Mei D, et al. Macrophage mediated biomimetic delivery system for the treatment of lung metastasis of breast cancer. *J Control Release*. 2015;204:11–19. doi:10.1016/j.jconrel.2015.01.039

30. Qiang L, Cai Z, Jiang WJ, et al. A novel macrophage-mediated biomimetic delivery system with nir-triggered release for prostate cancer therapy. *J Nanobiotechnol*. 2019;17(1):83. doi:10.1186/s12951-019-0513-z

31. Choi J, Kim HY, Ju EJ, et al. Use of macrophages to deliver therapeutic and imaging contrast agents to tumors. *Biomaterials*. 2012;33(16):4195–4203. doi:10.1016/j.biomaterials.2012.02.022